J Therm Anal Calorim (2009) 97:137–141
DOI 10.1007/s10973-009-0240-z

Structural and thermal characterization of $Zn_{2-x}Co_xTiO_4$

C. L. Santos · B. J. S. Capistrano · F. T. G. Vieira · M. R. C. Santos · S. J. G. Lima · E. Longo · C. A. Paskocimas · A. G. Souza · L. E. B. Soledade · I. M. G. Santos

ICTAC2008 Conference

Abstract In this work, spinels with the general formula $Zn_{2-x}Co_xTiO_4$ were synthesized by the polymeric precursor method and thermally treated at 1,000 °C. The powder precursors were characterized by TG/DTA. A decrease in the DTA peak temperature with the amount of zinc was observed. After the thermal treatment, the characterizations were performed by XRD, IR, colorimetry and UV/VIS spectroscopy. The XRD patterns of all the samples showed the presence of the spinel phase. Infrared spectroscopy showed the presence of ester complexes for Zn_2TiO_4 after thermal treatment at 500 °C, which disappeared after cobalt addition, indicating that organic material elimination was favored.

Keywords Spinel · Zn_2TiO_4 · Pigments · Cobalt · Polymeric precursor method

C. L. Santos (✉) · B. J. S. Capistrano · F. T. G. Vieira · M. R. C. Santos · A. G. Souza · L. E. B. Soledade · I. M. G. Santos
LACOM, Departamento de Química/CCEN, Universidade Federal da Paraíba, Campus I, CEP 58059-900, João Pessoa, PB, Brazil
e-mail: ieda@quimica.ufpb.br

S. J. G. Lima
LSR, Departamento de Engenharia Mecânica/CT, Universidade Federal da Paraíba, Campus I, João Pessoa, PB, Brazil

E. Longo
CMDMC—LIEC, Instituto de Química, UNESP, Araraquara, SP, Brazil

C. A. Paskocimas
Departamento de Engenharia Mecânica/CT, Universidade Federal do Rio Grande do Norte, Natal, RN, Brazil

Introduction

Composite oxides with spinel structure (AB_2O_4) are important inorganic materials being widely used in different fields. They are used as heat-resistant pigments, gas-sensors, catalysts, magnetic materials and wave absorption materials. Two types of spinel are usually observed, the normal and the inverse. Normal spinel compounds generally display the AB_2O_4 stoichiometry with A cations in tetrahedral sites and B cations in octahedral sites [1]. In inverse spinels, B cations are in octahedral sites, while A occupies both octahedral and tetrahedral sites [2]. Zinc titanate (Zn_2TiO_4) is an inverse spinel, with zinc located in tetrahedral and octahedral sites, while titanium only occupies octahedral sites.

The synthesis method has a great influence on the material properties, due to differences in particle morphology, homogeneity, and cation distribution in the sites. The conventional method of mixture of oxides has low reproducibility, purity and stoichiometric control. The chemical synthesis methods, including the method utilized, the polymeric precursor method, usually lead to better results, such as high stoichiometric precision, besides a good control of powder morphology [2–5].

In the polymeric precursor method, a polymeric chain is formed as a result of the reaction between a polyalcohol and a polycarboxylic acid. The cations are homogenously distributed throughout the polymeric chain. A thermal treatment at oxidizing conditions of this polymeric resin at 300 °C leads to the polymer breakage and a further heating leads to the oxide formation.

Titanate spinels have been successfully synthesized using the polymeric precursor method. Souza et al. [6] synthesized Zn_2TiO_4 doped with Co^{2+}, Ni^{2+}, Mn^{2+} and Fe^{3+}. Silva et al. [7] synthesized Mg_2TiO_4 with additions of Mn^{2+}, Fe^{3+} and Co^{2+}.

In this work, the Zn_2TiO_4 spinel with Co^{2+}-substitution for Zn^{2+} was synthesized by the polymeric precursor method, thus leading to the $Zn_{2-x}Co_xTiO_4$ (x = 0–2) stoichiometry. The thermal, structural, morphological and optical properties of this system were evaluated.

Experimental

In this work the following reagents were used in the synthesis: citric acid (Cargill), ethylene glycol (Vetec), zinc nitrate (Vetec), cobalt acetate (Vetec) and titanium isopropoxide (Hulls-AG). Titanium citrate was previously prepared according to the procedure described in the literature [6–8]. A 3:1 citric acid:metals molar rations were used.

The $Zn_{2-x}Co_xTiO_4$ (x = 0–2) pigments were synthesized using 60 mass% of citric acid to 40 mass% of ethylene glycol.

The powder precursors were characterized by thermal analysis, using a TA Instruments SDT 2960 simultaneous TGA-DTA analyzer at a heating rate of 10 °C min^{-1} up to 1,200 °C. The analyses were carried out in a synthetic air atmosphere with a flow rate of 110 mL min^{-1}. About 15 mg of sample mass was employed.

After calcination at 1,000 °C for 2 h, the materials were characterized by X-ray diffraction (D 5000—Siemens) with CuKα target; infrared spectroscopy (MB 102—Bomem), using KBr pellets; and VIS spectroscopy (Color-Eye 2180—Gretag Macbeth).

Results and discussion

The TG/DTG curves (Fig. 1, Table 1) present two thermal decomposition steps, the first one is assigned to the evaporation of water and adsorbed gases from the powder surface and the second step is due to the combustion of organic material, with CO_2 and H_2O evolution. The DTG curves indicate that the cobalt addition leads to an increase in mass loss at lower temperatures with the presence of a second DTG peak. This result indicates that cobalt leads to the presence of organic material with lower stability.

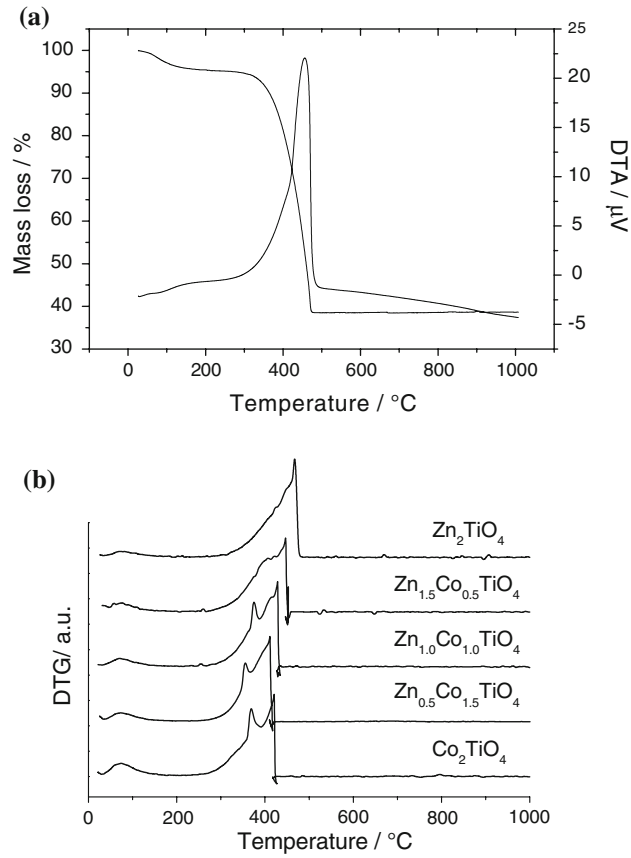

Fig. 1 Thermal analyses of the $Zn_{2-x}Co_xTiO_4$ (x = 0–2) precursors. **a** TG/DTA curve of the Zn_2TiO_4 sample and **b** DTG curves of all the samples

The DTA results indicate that the peak temperatures decrease with the increase of the amount of cobalt except for the Co_2TiO_4 precursor. This result is in agreement with the DTG peak temperatures. Gouveia et al. [9] synthesized the spinel $Co_xZn_{7-x}Sb_2O_{12}$ (x = 0–7) using also the polymeric precursor method and observed the same behavior.

Table 1 Temperatures and mass losses based on TG/DTG curves

Sample	Step	Temperature range (°C)	DTG peak temperatures (°C)	Mass loss (%)	Process
Zn_2TiO_4	1st	35–231	78	7.1	Endo
	2nd	231–497	470	55.0	Exo
$Zn_{1.5}Co_{0.5}TiO_4$	1st	31–264	74	6.6	Endo
	2nd	264–479	446	52.0	Exo
$ZnCoTiO_4$	1st	28–249	74	6.7	Endo
	2nd	249–500	376 and 427	55.2	Exo
$Zn_{0.5}Co_{1.5}TiO_4$	1st	30–205	74	7.0	Endo
	2nd	205–430	360 and 411	55.5	Exo
Co_2TiO_4	1st	27–203	74	10.0	Endo
	2nd	203–430	372 and 421	58.8	Exo

The infrared spectra of the $Zn_{2-x}Co_xTiO_4$ system, thermally treated at 500 and 1,000 °C are presented in Fig. 2. The increase in temperature leads to vibrational Me–O bands with better definition. All samples presented a band at 1,629 cm^{-1} after calcination at 500 °C, assigned to the (H–O–H) deformation vibration and it is an evidence of the presence of water molecules adsorbed on the surface of the powders [10]. This adsorption occurred because samples were not placed under special conditions after calcination.

According to Fig. 2a, its intensity decreases with the cobalt amount indicating that it may be related to organic material. Zn_2TiO_4 also presents bands at 1,564, 1,522, 1,382 and 1,004 cm^{-1}. The first three bands were assigned to C=O and C–O bands in ester complexes. The band at 1,004 cm^{-1} is probably due to the presence of water on the powder surface [10].

In Fig. 2a, the two vibration bands observed at 653 and 555 cm^{-1} present a higher definition with higher Co concentrations in such a way that at 100% Co these are the best defined bands. The vibration band in the 913–466 cm^{-1} region for the samples thermally treated at 1,000 °C, Fig. 2b was attributed to the spinel vibration modes. Due to equipment limitations, it was not possible to study the vibration bands for wavenumbers below 400 cm^{-1}.

The XRD patterns of the $Zn_{2-x}Co_xTiO_4$ pigments thermally treated at 1,000 °C are depicted in Fig. 3b. In the figure one can observe that the spinel phase was successfully synthesized using the polymeric precursor method. The phases are indexed based on the file JCPDS 00-002-1033 (Joint Committee on Powder Diffraction Standards).

Figure 3b shows that the samples with Co concentration of 25% and 50% are single phase. Secondary phases were observed for the pure Zn_2TiO_4 and Co_2TiO_4 samples and for the $Zn_{0.5}Co_{1.5}TiO_4$ sample. The XRD patterns of the Zn_2TiO_4 showed ZnO as secondary phase, with a peak at $2\theta = 33°$. For the $Zn_{0.5}Co_{1.5}TiO_4$ and Co_2TiO_4, samples peaks ascribed to $(Co,Zn)TiO_3$ were noticed. The Co_2TiO_4 sample, thermally treated at 500 °C (see Fig. 3a) displayed the Co_3O_4 phase. It should be noted that at 1,000 °C the peak related to this phase is not observed but the $CoTiO_3$ phase is still noted. Probably cobalt, which was added as Co^{2+}, was previously oxidized to Co^{3+} and at such higher temperature is reduced back to Co^{2+} [11].

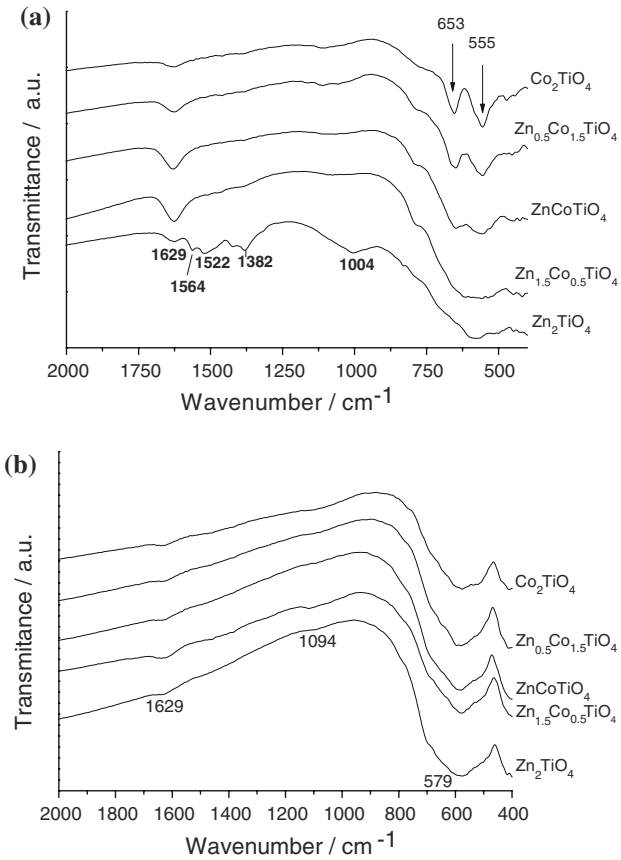

Fig. 2 Infrared spectra of $Zn_{2-x}Co_xTiO_4$ (x = 0–2) after calcination at: **a** 500 °C; **b** 1,000 °C

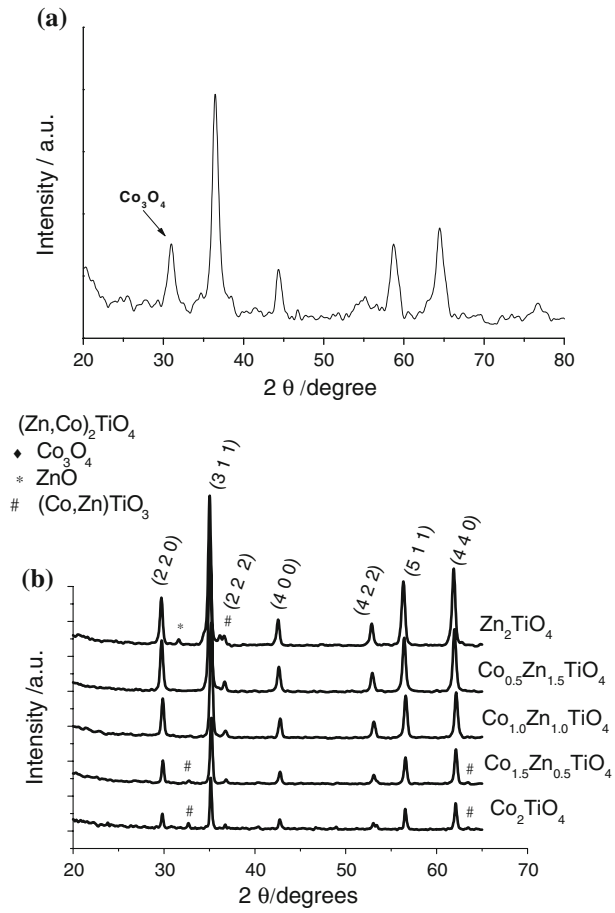

Fig. 3 XRD patterns of the samples: **a** Co_2TiO_4 at 500 °C and **b** $Zn_{2-x}Co_xTiO_4$ ($0.0 \leq x \leq 2.0$) at 1,000 °C

In Fig. 4a the FWHM values are displayed related to the (311) plane obtained in the XRD patterns of the $Zn_{2-x}Co_xTiO_4$ system, calcined at 1,000 °C as a function of the Co concentration. This figure shows that the sample with the highest long range organization is the $ZnCoTiO_4$ containing 50 mol% of both Co^{2+} and Zn^{2+}.

In spite of the similar values of ionic radii the decrease in the lattice parameter can be associated to the difference in the fillings of *d* orbitals in cobalt and zinc and not to the differences in these radii taking into account that Zn^{2+} displays its *d* orbitals completely filled and paired whereas Co^{2+} cobalt displays its *d* with seven electrons. With such difference in the *d* orbital fillings Zn^{2+} can cause a higher repulsion on the electrons of the neighbor oxygen atoms as compared with the repulsion caused by Co^{2+}, which presents a smaller electron density in its *d* orbitals. Thus the Co–O bond is smaller than the Zn–O bond, leading to smaller lattice parameters [12].

Figure 5a illustrates the absorbance in the 300–800 nm range for the $Zn_{2-x}Co_xTiO_4$ system samples treated at 1,000 °C. It can be observed that the Co-enrichment leads to a higher absorbance.

The values of bandgap energies, E_g were calculated by the Tauc method [13]. The results obtained are illustrated in Fig. 5b. The values decrease with the introduction of Co into the lattice but do not change markedly upon a further Co-enrichment in the lattice. Similarly to what was proposed in terms of lattice parameters the low electron repulsion between O and Co as compared with O and Zn may lead to a lower bond energy and thus to intermediate energy levels in the bandgap giving raise to lower bandgap energies. The breakage of symmetry and its consequent Jahn Teller effect will also contribute to lower bandgaps. The further Co-enrichment will not cause a further decrease in the bandgap as no other intermediate energy level will be created.

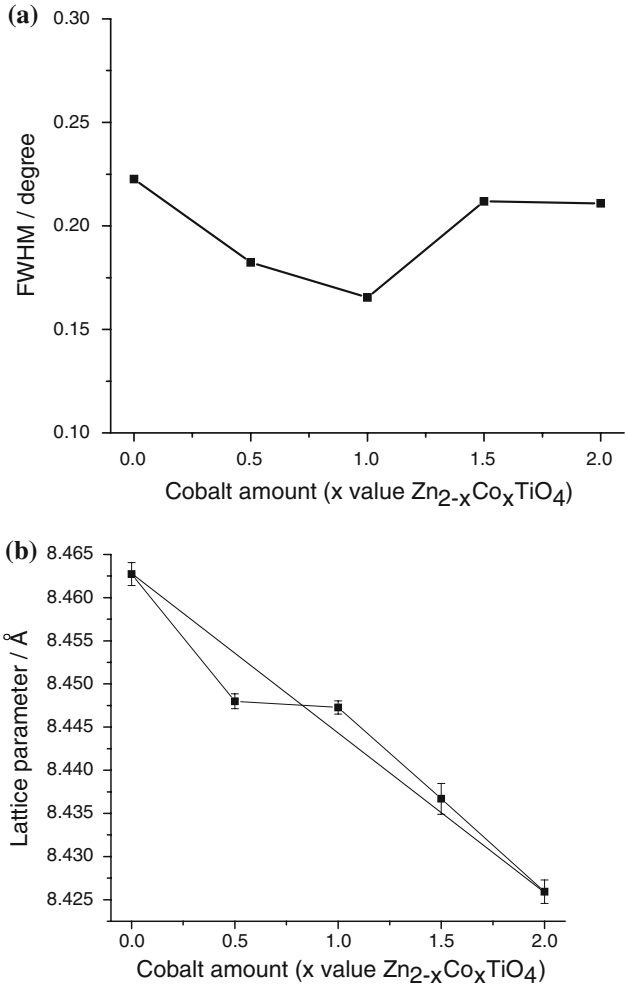

Fig. 4 Structure-related values of the $Zn_{2-x}Co_xTiO_4$ system, calcined at 1,000 °C. **a** FWHM. **b** Lattice parameter

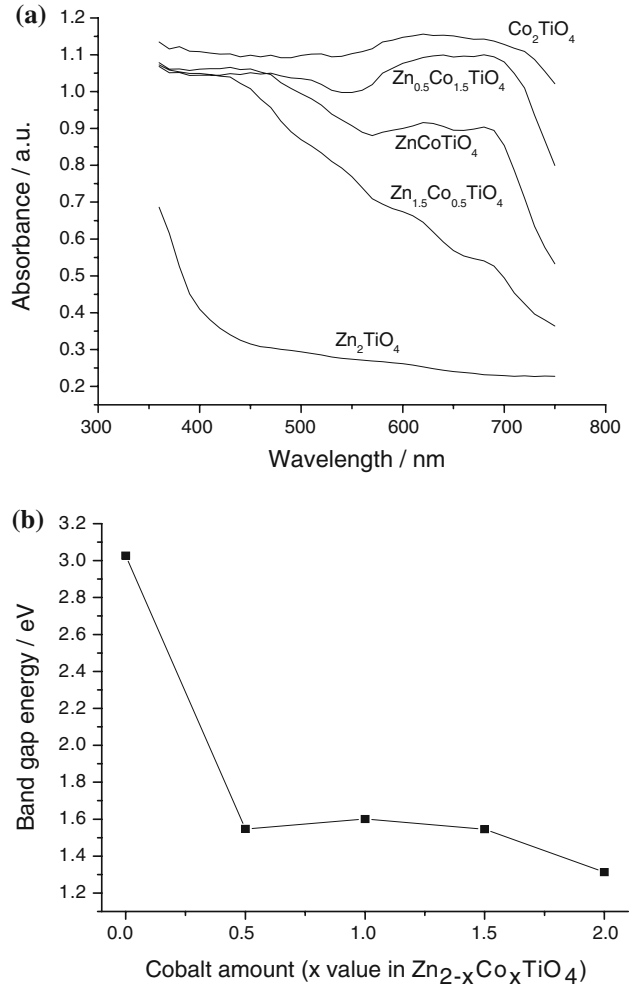

Fig. 5 Information obtained from the absorbance data. **a** Reflectance spectra of the $Zn_{2-x}Co_xTiO_4$ samples ($0 \leq x \leq 2$) treated at 1,000 °C. **b** Bandgap energies, calculated from the absorbance spectra

Conclusions

The DTG curves indicate that the cobalt addition leads to an increase in the amount of material eliminated at lower temperatures with the presence of a second DTG peak. This result indicates that cobalt leads to the presence of organic material with lower stability.

All samples presented a band at 1,629 cm^{-1} after calcination at 500 °C assigned to the (H–O–H) deformation vibration and it is an evidence of a great amount of water molecules adsorbed on the surface of the powders. Its intensity decreases with the amount of cobalt indicating that it may be related to organic material.

In agreement with the DTA analyses the higher temperature peak for the $Zn_{2-x}Co_xTiO_4$ system may be related to the combustion of ester complexes.

The XRD patterns of the $Zn_{2-x}Co_xTiO_4$ pigments thermally treated at 1,000 °C show that the spinel phase was successfully synthesized using the polymeric precursor method, although secondary phases were observed in some samples.

For the $Zn_{2-x}Co_xTiO_4$ system thermally treated at 1,000 °C the absorbance in the 300–800 nm range increases with the Co-enrichment.

The values of bandgap energies decrease with the introduction of Co into the lattice, but do not change markedly upon a further Co-enrichment in the lattice. Similarly to what was proposed in terms of lattice parameters the low electron repulsion between O and Co as compared with O and Zn may lead to a lower bond energy and, thus, to intermediate energy levels in the bandgap giving raise to lower bandgap energies. The breakage of symmetry and its consequent Jahn Teller effect will also contribute to lower bandgaps. The further Co-enrichment will not cause a further decrease in the bandgap as no other intermediate energy level will be created.

References

1. Müller-Buschbaum Hk. The crystal chemistry of AM_2O_4 oxometallates. J Alloy Compd. 2003;349:49–104.
2. Leite ER, Souza CMG, Longo E, Varela JÁ. Influence of the polymerization on the synthesis of $SrTiO_3$: Part I, characteristics of the polymerics precursors and its thermal decomposition. Ceram Int. 1995;21:143–52.
3. Pechini MP. US Patent, No. 3.330.697 (1967).
4. Alves MCF, Souza SC, Lima SJG, Longo E, Souza AG, Santos IMG. Influence of the precursor salts in the synthesis of $CaSnO_3$ by the polymeric precursor method. J Therm Anal Calorim. 2007;87:763–6.
5. Silva MRS, de Miranda LCO, Cassia-Santos MR, Lima SJG, Soledade LEB, Longo E, et al. Influence of the network former on the properties of magnesium spinels. J Therm Anal Calorim. 2007; 87:753–7.
6. Souza SC, Souza MAF, Lima SJG, Santos MRC, Fernandes VJ Jr, Soledade LEB, et al. The effects of Co, Ni and Mn on the thermal processing of Zn_2TiO_4 pigments. J Therm Anal Calorim. 2005;79:455–9.
7. Silva MRS, Souza SC, Santos IMG, Santos MRC, Soledade LEB, Souza AG, et al. Stability studies on undoped and doped Mg_2TiO_4 obtained by the polymeric precursor method. J Therm Anal Calorim. 2005;79:421–4.
8. Souza MAF, Candeia RA, Lima SJG, Santos MRC, Santos IMG, Longo E, et al. Thermal and structural characterization of $Sr_{1-x}Co_xTiO_3$ obtained by polymeric precursor method. J Therm Anal Calorim. 2005;79:407–10.
9. Gouveia DS, Rosenhaim R, Lima SJG, Longo E, Souza AG, Santos IMG. The characterization of $Co_xZn_{7-x}Sb_2O_{12}$ spinel obtained by the Pechini method. Mater Res. 2005;8:213–9.
10. Nakamoto K. Infrared and Raman spectra of inorganic and coordination compounds. New York: Willey; 1986.
11. Dibb A, Tebcherani SM, Lacerda W Jr, Santos MRC, Cilense M, Varela JA, et al. Influence of simultaneous addition of MnO_2 and CoO on properties of SnO_2-based ceramics. Mater Lett. 2000;46: 39–43.
12. Chiang YM, Birnie DIII, Kingery WD. Physical ceramics—principles for ceramic science and engineering. New York: Wiley; 1997.
13. Wood DL, Tauc J. Weak absorption tails in amorphous semiconductors. Phys Rev B. 1972;5:3144–51.